Experimental Comparison of Synchronous-Clock Cooperative Acoustic Navigation Algorithms

Jeffrey M. Walls*, Ryan M. Eustice†
Department of Mechanical Engineering*
Department of Naval Architecture and Marine Engineering†
University of Michigan, Ann Arbor, Michigan 48109
Email: {jmwalls,eustice}@umich.edu

***Abstract*—This paper reports on an experimental comparison of three synchronous clock, acoustic, distributed navigation algorithms commonly found in the underwater robotics community and literature: a naively distributed extended Kalman filter (NEKF), the interleaved update (IU) algorithm, and a decentralized extended information filter (DEIF). Traditional dead-reckoned underwater navigation methods result in unbounded error growth as subsea vehicles do not typically have access to an absolute position reference. Synchronous-clock acoustic navigation systems can provide one-way travel time (OWTT) range constraints to nearby vehicle nodes thereby bounding error. Several distributed estimation algorithms for such scenarios have been proposed by the community; however, each makes fundamentally different trade offs in various specifications such as scalability, complexity, directionality, and consistency. We report an experimental comparison between the performance of each algorithm as compared to the benchmark solution of a centralized extended Kalman filter (CEKF) applied to a variety of 2-node and 3-node vehicle network topologies using data collected from two Ocean-Server autonomous underwater vehicles (AUVs) and a surface craft.**

I. Introduction

Typical advanced navigation sensor suites for underwater vehicles are capable of measuring Doppler body-frame velocity, MEMS/gyro attitude, and pressure depth. Integrating these measurements over time results in so-called dead-reckoned (DR) navigation solutions, which produce position estimates whose error grows unbounded with time. The strong attenuation of electromagnetic (EM) signals underwater precludes the use of GPS (except for at the surface), which is frequently used to bound pose-error growth in terrestrial and aerial navigation scenarios. Higher quality DR sensors are only capable of reducing the rate of uncertainty growth, therefore, alternative methods for constraining navigation errors are required.

Underwater acoustic navigation systems attain bounded-error navigation through range-only observations to beacons with known position. Range observations are derived from measuring the time-of-flight (TOF) of acoustic signals and assuming a well known sound speed profile. The long-baseline (LBL) navigation framework, for example, employs a network of fixed reference beacons to which vehicles can measure range [1]. LBL, however, limits the area of operations to the coverage footprint of the reference beacons. Furthermore, narrowband LBL lacks the ability to scale up to large groups of vehicles because only a single vehicle can interrogate the beacon network at any one time.

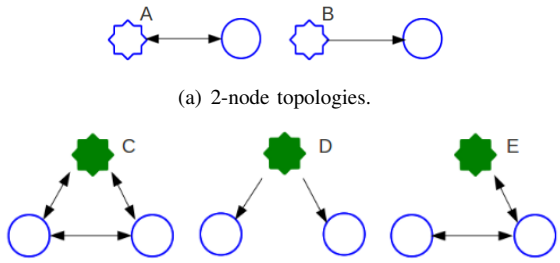

(a) 2-node topologies.

(b) 3-node topologies.

Fig. 1. An depiction of the 2-node and 3-node topologies studied in this experiment. The arrows in each image represent the direction of communications (i.e., unidirectional versus bidirectional). Stars indicate that an absolute position reference (e.g., GPS or LBL) was available at some point during the mission while circles represent nodes without absolute position reference. Subsea and topside nodes are color coded by blue and green, respectively.

Synchronous-clock acoustic navigation [2] is an alternative method in which receiving nodes are able to measure one-way travel time (OWTT) range to a transmitting node. Advantageously, synchronous-clock acoustic networks scale to arbitrarily many vehicles because all vehicles within acoustic range of the transmitting node passively receive a range measurement leading to constant time update rates.

A variety of estimation frameworks have been introduced for incorporating acoustic ranging to nodes with known but non-stationary position. The moving long-baseline (MLBL) navigation approach [3] allows vehicles with high-quality navigation sensors to act as position references to vehicles with less accurate navigation systems. [2] proposes a maximum likelihood estimate (MLE) solution for synchronously navigating subsea nodes via ranging to surface ships. Multiple navigation systems framed around the Kalman family of filters have been proposed and consider ranging between all acoustic nodes [4–6]. We consider this scenario of synchronous-clock acoustic navigation incorporating range measurements across an acoustic network.

In this work, we seek to benchmark existing algorithms for synchronous-clock cooperative underwater navigation from within the associated literature and throughout the community. Representative network topologies considered in this study are illustrated in Fig. 1. As our benchmark we report a comparison

of a post-process centralized extended Kalman filter (CEKF) approach [4] to a naively distributed extended Kalman filter (NEKF), to a decentralized extended information filter (DEIF) [7] and to the interleaved update (IU) algorithm [6]. Section II formalizes the problem statement and reviews each of the algorithms. Section III presents a multi-vehicle experiment sharing inter-node ranges and discusses the performance of each filter. Section IV offers a discussion of the various filter performances and Section V closes with concluding remarks.

II. Cooperative Underwater Navigation

We define the general problem of cooperative underwater navigation simply as estimating position by measuring range relative to other nodes. Furthermore, we make the following assumptions:

1) the motion of each node can be described by independent linear dynamics;
2) all nodes carry a sensor suite comprised of Doppler velocity log (DVL), attitude, and depth for DR;
3) attitude and depth are sufficiently well instrumented so that we can only consider XY horizontal position estimation, as range measurements can easily be projected to the local-level plane;
4) each node is equipped with an acoustic modem and a synchronous clock enabling the exchange of information and OWTT measurements.

Underwater acoustic networks are constrained by the physical communication layer and therefore message size is required to fit limited bandwidth. In addition, the acoustic channel is extremely susceptible to dropped transmission [8] requiring that a viable navigation framework should be robust to packet loss.

For this discussion, the state and distribution of the i^{th} vehicle are modeled as

$$\mathbf{x}_i = [x_i,\, y_i,\, \dot{x}_i,\, \dot{y}_i]^\top \quad \mathbf{x}_i \backsim \mathcal{N}(\mathbf{x}, \mathrm{P}) \tag{1}$$

where the vehicle position in the local-level plane is denoted by the xy pair and the corresponding world-frame velocities are $\dot{x}\dot{y}$. Each vehicle state is estimated assuming a constant velocity linear kinematic plant process model and a general nonlinear observation model

$$\dot{\mathbf{x}}_i(t) = \mathrm{F}_i(t)\mathbf{x}_i(t) + \mathbf{w}(t) \tag{2}$$

$$\mathbf{z}_i(t) = h(\mathbf{x}_i(t)) + \mathbf{v}(t) \tag{3}$$

with measurement $\mathbf{z}_i$, where velocity and global positioning system (GPS) observations are linear and OWTT are nonlinear. Each model is corrupted by time-independent, zero-mean, Gaussian noise $\mathbf{w}(t) \backsim \mathcal{N}(0, \mathrm{Q}(t))$ and $\mathbf{v}(t) \backsim \mathcal{N}(0, \mathrm{R}(t))$.

The state and covariance of each vehicle are propagated forward in time through a constant velocity linear kinematic model. After performing a standard discretization of a continuous linear system, the discrete time process prediction for estimated state and covariance follows

$$\hat{\mathbf{x}}_i(k+1|k) = \mathrm{F}_{i_k}\hat{\mathbf{x}}_i(k|k), \tag{4}$$

$$\mathrm{P}_i(k+1|k) = \mathrm{F}_{i_k}\mathrm{P}_i(k|k)\mathrm{F}_{i_k}^\top + \mathrm{Q}(k), \tag{5}$$

where using standard convention, $k+1|k$ represents the estimate of the state at time $k+1$ given state up through time k.

The measurement updates for local observations follow the standard Kalman update equations; however, each filtering scheme handles OWTT range measurement updates differently. Nonetheless, they all share the same measurement model, i.e., that the range measurement between vehicle i at the time-of-arrival (TOA) and vehicle j at the time-of-launch (TOL) can be modeled as

$$z_{\text{OWTT}} = \|\mathbf{x}_i(t_{\text{TOA}}) - \mathbf{x}_j(t_{\text{TOL}})\| + v_{\text{OWTT}} \tag{6}$$

where the measurement noise, $v_{\text{OWTT}} \backsim \mathcal{N}(0, \mathrm{R}_{\text{OWTT}})$, accounts for timing error multiplied by the speed of sound.

A. Centralized Extended Kalman Filter Implementation

We first consider the implementation of the CEKF, which serves as our benchmark "gold-standard" solution [4]. The CEKF is a post process formulation that has access to all sensor measurements from all nodes. Initially, the navigation estimates of each vehicle are uncorrelated so that the global covariance matrix is block diagonal. However, sharing inter-node range measurements builds correlation between vehicle navigation estimates (see Appendix A). The power of the CEKF is that it is able to track the fully dense covariance matrix of the network, whereas real-time decentralized implementations are, in general, unable to do so as they are constrained by limited bandwidth.

The CEKF tracks the global state composed of the stacked state and covariance of all n-vehicles in the network:

$$\mathbf{x} = \begin{bmatrix} \mathbf{x}_1 \\ \mathbf{x}_2 \\ \vdots \\ \mathbf{x}_n \end{bmatrix} \quad \mathrm{P} = \begin{bmatrix} \mathrm{P}_{11} & \dots & & \mathrm{P}_{1n} \\ \vdots & \mathrm{P}_{22} & & \vdots \\ & & \ddots & \\ \mathrm{P}_{n1} & \dots & & \mathrm{P}_{nn} \end{bmatrix}.$$

The state and covariance follow the standard Kalman prediction equations with a combined state transition matrix, F, and noise covariance matrix, Q, given by

$$\mathrm{F} = \mathrm{blkdiag}(\mathrm{F}_1, \mathrm{F}_2, \dots, \mathrm{F}_n)$$

$$\mathrm{Q} = \mathrm{blkdiag}(\mathrm{Q}_1, \mathrm{Q}_2, \dots, \mathrm{Q}_n).$$

In order to correctly model range measurement updates, the CEKF augments the global state to include the transmitting node at the TOL,

$$\mathbf{x}' = [\mathbf{x}_1^\top, \mathbf{x}_2^\top, \dots, \mathbf{x}_n^\top, \mathbf{x}_{\text{TOL}}^\top]^\top.$$

This allows the filter to perform a standard nonlinear Kalman update with the OWTT observation as written in (6). Once the measurement update has been carried through, the augmented state can be marginalized out in order to maintain a bounded state size.

B. Naively Distributed Extended Kalman Filter

The NEKF approach is essentially equivalent to the CEKF with all of the off block-diagonal elements of the covariance matrix actively held zero. Distributing this filter only requires that local state and covariance, $\hat{\mathbf{x}}_i$ and P_i, respectively, be transmitted by any source node. Acoustic data packets are constant size as only local information is transmitted. Therefore, the NEKF can trivially scale up to arbitrarily large networks. However, this real-time method trades simple application for an inconsistent (i.e., overconfident) estimate because inter-node correlation is not tracked.

In order to perform a range measurement update, the receiving node, j, constructs a combined state vector and covariance matrix by appending the statistics of the transmitting node, i.

$$\mathbf{x}' = \begin{bmatrix} \mathbf{x}_i \\ \mathbf{x}_j \end{bmatrix} \quad \mathrm{P}' = \begin{bmatrix} \mathrm{P}_i & 0 \\ 0 & \mathrm{P}_j \end{bmatrix}.$$

The measurement update then proceeds with the standard Kalman update with measurement model given in (6). Following the update, the state elements corresponding to the transmitting node, i, are marginalized out. Note that this filter does not track correlation; when j transmits to i, i will use the same update procedure assuming no correlation, resulting in a double-counting of information as j's state was previously informed by i's.

C. Interleaved Update Algorithm

Bahr et al. [6] proposed the IU algorithm as a solution to the problem of inconsistency in position estimates between nodes exchanging navigation information. To avoid overconfidence, the IU algorithm only performs range measurement updates between vehicle navigation estimates that are known to be uncorrelated. While the IU algorithm is essentially a book keeping utility that can be wrapped around a variety of filtering modalities (e.g., extended Kalman filter (EKF), particle filter, unscented Kalman filter (UKF)), for comparison with the other acoustic navigation frameworks considered in this paper, we present the IU as applied to an EKF.

Each node maintains a bank of EKFs with an index of the origins of each measurement. The set of state vectors and covariance matrices at time k tracked by the i^{th} node, denoted $\mathcal{X}_i(k)$ and $\mathcal{P}_i(k)$, respectively are defined as

$$\mathcal{X}_i(k) = \{\mathbf{x}_i^1(k), \mathbf{x}_i^2(k), \ldots, \mathbf{x}_i^{2n-1}(k)\},$$
$$\mathcal{P}_i(k) = \{\mathrm{P}_i^1(k), \mathrm{P}_i^2(k), \ldots, \mathrm{P}_i^{2n-1}(k)\},$$

where n is the total number of vehicles in the network.

In order to track the origins of each acoustic broadcast, all nodes retain a transmission matrix T where each row represents a filter within its local set and each column corresponds to a vehicle in the network. Hence, each T_{ij} entry represents the last time that the i^{th} filter used the j^{th} vehicle to update its navigation estimate.

Under the IU framework, each source node acoustic transmission encodes the transmission matrix as well as its entire bank of filters. A receiving node updates each of its filters by searching for a corresponding filter in the transmitted set that does not contain an update that could be correlated. The full mechanics of this update step are detailed in [6]. It is this combinatorial nature of the IU algorithm that ensures that double counting of information will not occur where correlation could exist.

D. Decentralized Extended Information Filter Method

Webster et al. [7] report a distributed algorithm that exactly reproduces the CEKF by adding a few extra constraints on the vehicle network topology and system dynamics. The key insight comes from working with the additive updates available in the information form of the Kalman equations, resulting in what is called a DEIF.

Their assumptions limit networks to tree-connected topologies and force the root of each tree to evolve with linear predictions and updates. In this scenario the root of each tree cooperatively navigates each of the leaf nodes by acting as a moving reference beacon. By encoding "delta information" into each acoustic packet, the receiving nodes can *exactly* reconstruct the distribution tracked by the CEKF.

The interested reader is referred to [7] for full details pertaining to transmitting and receiving delta information. Essentially, the transmitting node maintains its current state as well as delayed-states corresponding to TOLs. The receiving node tracks its current state in addition to the TOL states of the transmitting node. The delta information packets summarize all predictions and observations that have occurred since the last TOL by the root node allowing the receiving node to track the state of the transmitting node. Furthermore, the receiving node filter is able to build correlation in its estimate with the transmitting node resulting in a consistent estimate that matches the CEKF at the time of packet integration.

III. Experiments

A. Experimental Setup

A multi-node autonomous underwater vehicle (AUV) trial was carried out for a three-node network topology. The experiment consisted of two custom modified Ocean-Server, Inc. Iver AUVs operated by the Perceptual Robotics Laboratory (PeRL) at the University of Michigan and a topside surface craft. Each AUV followed a lawn-mower pattern with roughly 500 m tracklines spaced 50 m apart as depicted in Fig. 2. The topside ship traveled to various positions around the survey area during the mission.

The two AUVs, referred to as Iver28 and Iver31, contain a typical advanced DR AUV sensor suite as detailed in [9]. Each AUV measured body-frame velocities with a 600 kHz RDI DVL, attitude with a Microstrain 3DM-GX1-AHRS, and depth with a Desert Star Systems SSP-1 digital pressure sensor. Since we consider attitude to be well instrumented with bounded error, we project the body-frame velocity measurements into the world-frame and treat these as linear observations of the $\dot{x}$ $\dot{y}$ elements of our state. The topside vehicle only observes world-frame position measured by GPS.

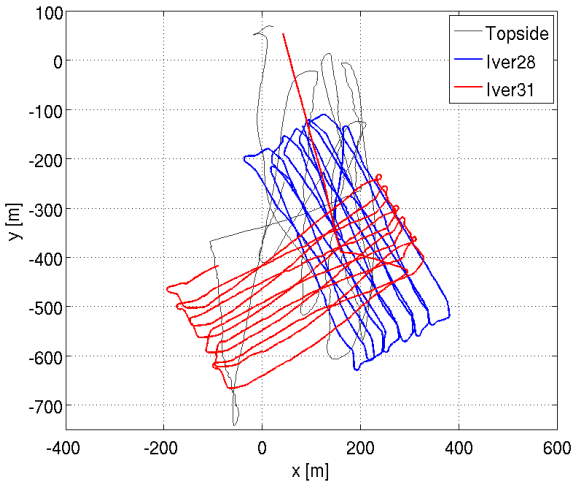

(a) AUV and topside trajectories.

(b) One of two Iver AUVs used in field experiments.

Fig. 2. The top plot shows the trajectories of the two AUVs and the topside surface ship. The lower figure depicts one of the AUVs.

The source of each acoustic transmission was defined by a fixed time division multiple access (TDMA) schedule during which each vehicle was assigned a time-slot to send a data packet. The network maintained a 145 second TDMA cycle, which consisted of 6 topside broadcasts and 4 subsea broadcasts from each AUV.

B. Vehicle Network Topologies

We compared the performance of each of the filtering schemes through post-process implementation. Since the data sets are bidirectional, time-synchronized and recorded to disk, we were able to selectively ignore certain OWTT measurements in order to artificially create different network topologies, as depicted in Fig. 1.

Two two-node experiments were run with the two AUVs exchanging information as depicted in Fig. 1(a). Both Iver28 and Iver31 communicate bidirectionally in topology A and unidirectionally in topology B where Iver28 supports Iver31. In both experiments, neither vehicle had access to an absolute position reference save for a short surface interval midway through the mission when Iver28 received several GPS measurements. Note that the AUV acoustic modem sits on the top of the nose cone, as seen in Fig. 2, so that the nodes cannot transmit or receive acoustic messages during surfacings due to the lack of an acoustic coupling.

Three experiments were executed for a three-node vehicle network consisting of a topside node and the two AUVs as illustrated in Fig. 1(b). In these experiments only topside received absolute position observations via GPS. Topology C represents the fully-connected case in which communication is shared among all vehicles. Topology D is representative of the common situation where a topside vessel supports multiple subsea vehicles. The last topology considered, E, limits communication to pairs of vehicles such that bidirectional communication links exist only between topside and Iver28 and between Iver28 and Iver31. In this case, we try to localize one subsea node from another subsea node in a cascaded cooperative navigation network.

C. Results

1) 2-Node Topology: The uncertainty estimates for both AUVs and their correlation from the two-node topology experiments are shown in Fig. 3. In both experiments, the NEKF reports an estimate of position uncertainty that is inconsistent with that reported by the CEKF. These experiments also show that relative range measurements between the two vehicles build correlation between their navigation estimates. Note that the correlation is greatly reduced when Iver28 receives a GPS measurement midway through the experiment. The DEIF navigation estimate onboard Iver31 matches the CEKF estimate to numerical precision as seen in Fig. 3(b). Iver31's DEIF uncertainty estimate diverges briefly from the CEKF in this two node experiment, shown close up in Fig. 3(b). This period corresponds to a surface interval by Iver28. Once surfaced, Iver28 observes absolute position, which immediately drives the uncertainty down for both vehicles (Iver28 and Iver31) in the CEKF, however it is not until the next acoustic broadcast from the support vehicle (Iver28) that the subsea node's DEIF is able to fully incorporate the delta information with GPS and fully match the CEKF. Since Iver28 is the support node in the second two-node experiment and receives no acoustic broadcasts from Iver31, its NEKF, IU and DEIF navigation solutions are all equal as they only process local observations.

2) 3-Node Topology: Results for each AUV for all three-node topology experiments are shown in Fig. 4. We see that correlation computed within the CEKF framework between Iver28 and Iver31 does not persist as in the two-node case due to frequent topside GPS measurements. Note that correlation develops in the CEKF between both AUVs through the topside node, even in the experiment corresponding to topology D (Fig. 4(b)) where neither AUV directly communicates. The NEKF navigation uncertainty estimate for each vehicle more closely follows the CEKF, although still frequently overconfident. The DEIF does not exactly reproduce the CEKF output in the experiment corresponding to topology D (though unnoticeable at this scale); however, this is to be expected because a small amount of correlation develops between the leaf nodes that the DEIF is ignorant of. Unlike the CEKF in this topology, the DEIF only models interaction between pairs of vehicles, not the entire network. The cascaded navigation network performs well as Iver28 (communicating with the topside node) is able to effectively localize and bound the uncertainty of Iver31.

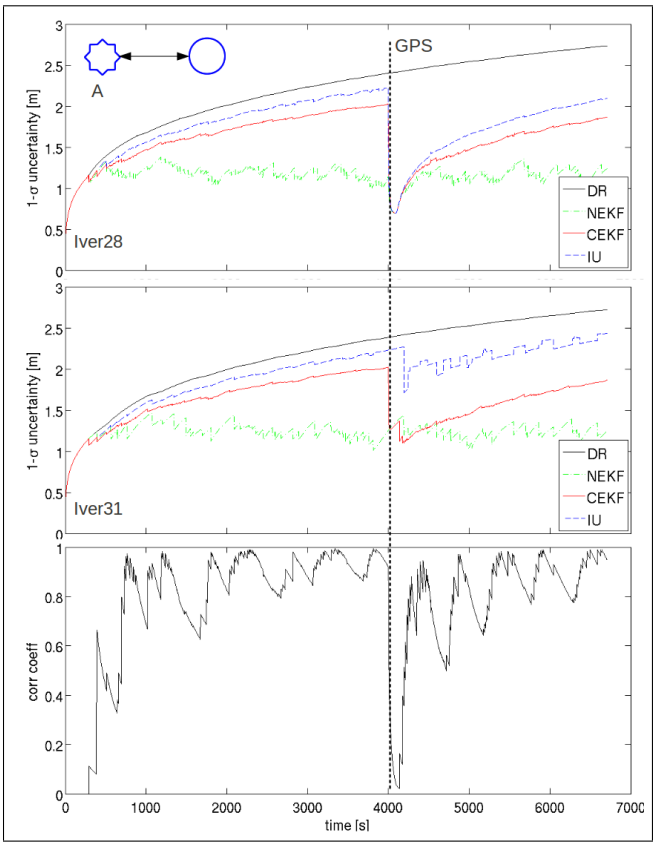

(a) Topology A: bidirectional 2-node network.

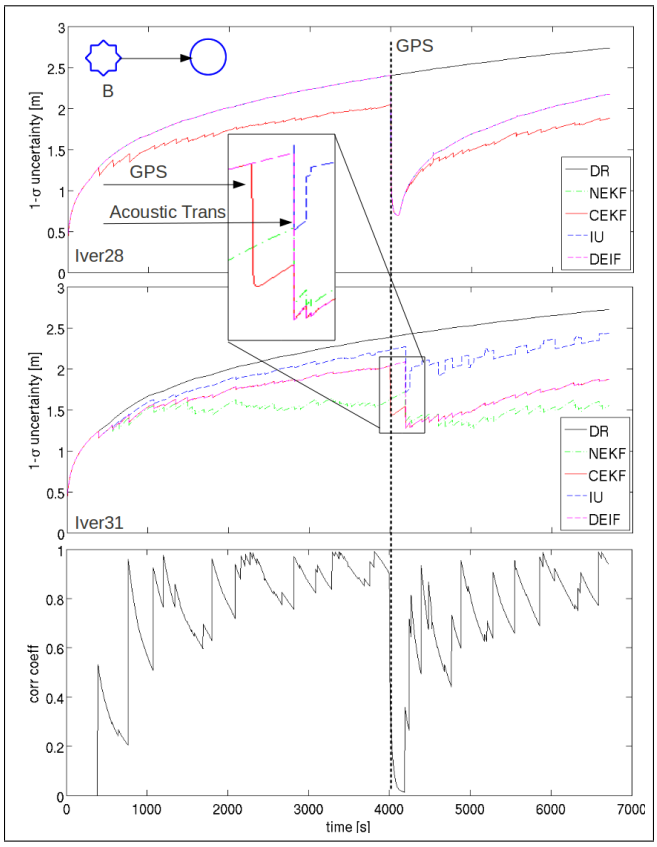

(b) Topology B: unidirectional 2-node network.

Fig. 3. The above plots show the 1-σ position uncertainty growth of Iver28 and Iver31 as computed by the different filters, and the true correlation that develops between the two subsea nodes as computed by the CEKF during a 2-node experiment. Halfway through the mission Iver28 receives GPS measurements during a brief surface interval. (a) corresponds to the case of a bidirectional communication link while (b) limits the topology to one-way communication.

TABLE I
DISTRIBUTED FILTER COMPARISON (✓= YES, X = NO)

	CEKF	**NEKF**	**IU**	**DEIF**
Consistent	✓	X	✓	✓
Bounds Error	✓	✓	X	✓
Arbitrary Network Topology	✓	✓	✓	X
Real-time	X	✓	✓	✓
Robust to dropped packets	✓	✓	✓	X
Number of floats per packet	N/A	6	1 + 4 per filter	15
Comments	realizable in post-process only	fixed bandwidth independent of network size	guaranteed to be consistent for any network topology	exactly reproduces CEKF in 2-node unidirectional topologies

IV. DISCUSSION

A comparison of the different filter characteristics is summarized in Table I and discussed in further detail below.

A. NEKF

The experiments clearly show that the NEKF fails most drastically to produce an estimate consistent with the CEKF within topologies where large correlation persists. For example, relative range measurements create large correlation between the two subsea nodes. Contrastingly, absolute position observations tend to destroy correlation between previously correlated nodes. Refer to Appendix A for a simplified example illustrating this phenomenon.

B. IU Algorithm

In general, we observe that the IU EKF shows improvement over DR. Although the estimate is consistent, the result still leads to unbounded uncertainty growth. This is due to the mechanism IU employs to ensure measurement updates are not performed using pose estimates that are correlated. We can easily see this in the two-node case. Each vehicle maintains

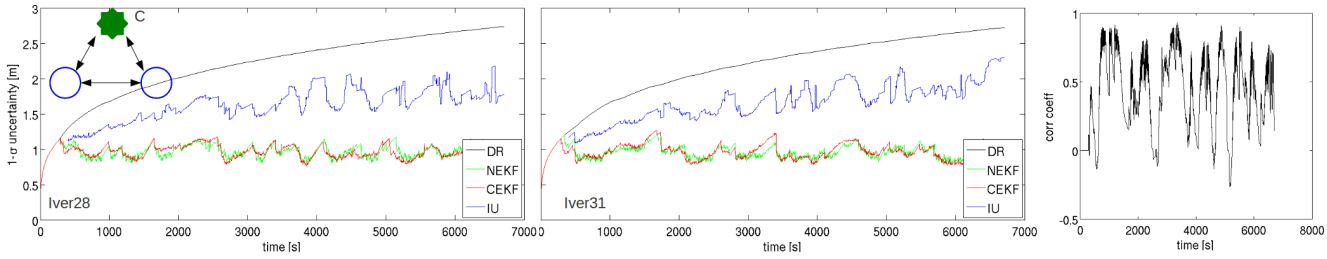

(a) Topology C: fully connected network.

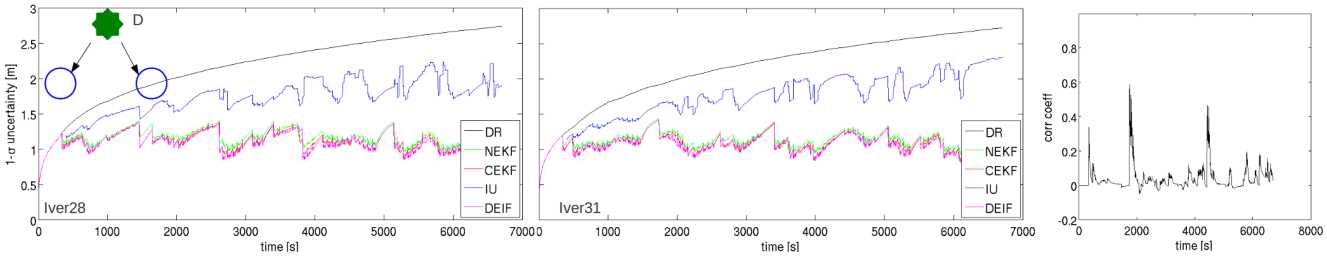

(b) Topology D: single support node with uni-directional communication links.

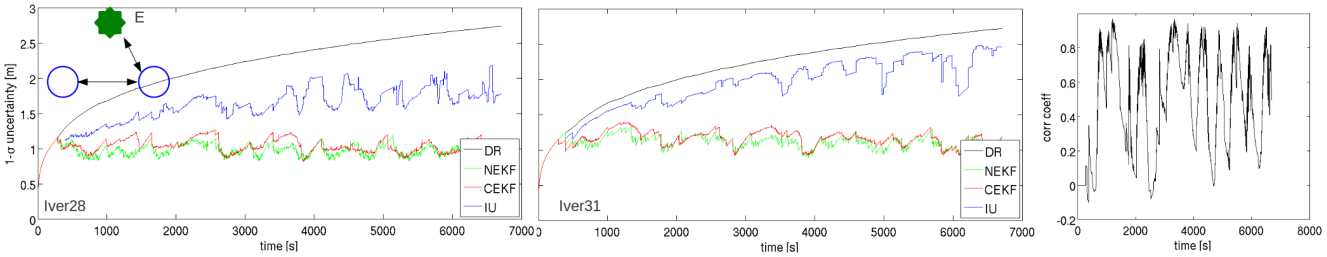

(c) Topology E: cascaded support navigation network.

Fig. 4. Each subfigure displays Iver28 and Iver31 1-σ position uncertainty as computed by the different filters and the true correlation between their position estimates as computed by the CEKF within a 3-node acoustic network. (a) corresponds to a fully-connected network. Only topside transmits in the experiment corresponding to (b). (c) displays the cascaded support navigation topology.

two filters: a filter that only processes local measurements and a filter incorporating range measurements. To avoid correlation, the second filter always uses the estimates from each vehicle that have only included local observations (DR for vehicles without access to an absolute position reference) to integrate a new range measurement. The unbounded uncertainty growth that develops with the IU is shown in all experiments, though improvement over DR is clear.

C. DEIF

Due to the assumptions of the DEIF, this filter is only applicable to two-node unidirectional topologies where one vehicle navigates a second. The DEIF performance in these cases, however, matches the CEKF exactly immediately upon incorporating delta information packets.

D. Filter Bandwidth Considerations

For completeness, we include a brief outline of the bandwidth requirements of each algorithm because of the severe bandwidth constraints imposed on data packet size by the acoustic channel. The relative data packet size demanded by each filter is summarized in Table I. We place a small overhead on each transmission by including depth information because we project range measurements into the local-level plane. The NEKF only requires that local state and covariance corresponding to xy position be encoded. Since symmetry is a property of covariance matrices, it is only necessary to transmit the upper diagonal elements. Therefore, the NEKF requires that 2 floats for state and 3 for covariance are transmitted. Since delta state in the DEIF is computed between the last TOL augmented state and the current xy position, the DEIF requires 4 floats for the delta information vector and 10 for the delta information matrix to be encoded in each data packet. The DEIF relies on a lossless communication network to correctly reassemble delta information packets. Practically this is not achievable, so a working implementation would require added bandwidth for increasing robustness, perhaps through sending the last k delta information packets [10]. Since the IU algorithm transmits its entire bank of filters, packet size is variable. In addition to encoding the transmission matrix, IU requires 2 floats for state and 3 for covariance (as each filter is a NEKF) be sent per filter. In a two-node network, for example, each vehicle must maintain three filters requiring 15 floats to transmit the filter set.

V. Conclusions and Future Work

We have presented a comparison of various filtering mechanisms for incorporating range-only measurements into an underwater position estimation framework. Through application to real-world data sets, we have shown the benefits and shortfalls of each algorithm. The attributes of each examined algorithm are summarized in Table I. Filter selection for an application depends on mission specifications such as network topology, sensor suite, and computational resources available on each vehicle. Future work in this area will be toward an algorithm that combines the best of all worlds, i.e. small bandwidth requirements with a consistent estimate that uses all information available, thereby continuing to leverage the benefits of synchronous-clock acoustic navigation networks.

VI. Acknowledgments

This work was supported by the National Science Foundation under awards IIS-0746455 and ANT-1039951, and by the Naval Sea Systems Command through the Naval Engineering Education Center under award N65540-10-C-0003. We are grateful to the University of Michigan Biological Station for their logistical support during field experiments.

Appendix

To demonstrate how absolute and relative position observations affect correlation between vehicles in a CEKF, we refer to a 2-node single degree of freedom (i.e., monobot) example. Two monobots exist on a line with global state $\mathbf{x}_g = [x_A, \dot{x}_A, x_B, \dot{x}_B]^\top$. We represent the state vector and covariance of this system after marginalizing out $\dot{x}_A$ and $\dot{x}_B$, which does not affect the shown result, by

$$\mathbf{x} = \begin{bmatrix} x_A \\ x_B \end{bmatrix} \quad \Sigma = \begin{bmatrix} \sigma_a^2 & \rho_{ab}\sigma_a\sigma_b \\ \rho_{ab}\sigma_a\sigma_b & \sigma_b^2 \end{bmatrix}$$

where the two monobot states initially have some arbitrary correlation coefficient ρ_{ab}.

This multi-monobot system occasionally observes the absolute location of the first vehicle with the following measurement model:

$$z = \mathrm{H}\mathbf{x} + v, \quad \mathrm{H} = \begin{bmatrix} 1 & 0 \end{bmatrix}$$

with measurement noise $v \backsim \mathcal{N}(0, \sigma_r^2)$.

Applying the standard Kalman update equations results in the new covariance matrix:

$$\Sigma' = \begin{bmatrix} \sigma_a^2\big(1 - \frac{\sigma_a^2}{\sigma_a^2+\sigma_r^2}\big) & \rho_{ab}\sigma_a\sigma_b\big(1 - \frac{\sigma_a^2}{\sigma_a^2+\sigma_r^2}\big) \\ \rho_{ab}\sigma_a\sigma_b\big(1 - \frac{\sigma_a^2}{\sigma_a^2+\sigma_r^2}\big) & \sigma_b^2\big(1 - \frac{\rho_{ab}^2\sigma_a^2}{\sigma_a^2+\sigma_r^2}\big) \end{bmatrix}.$$

From the updated covariance matrix, we observe that the variance in the location of the first robot as well as the correlation between the two robots is driven down for any finite measurement noise σ_r. Moreover, the variance σ_b^2 is reduced for any non-zero correlation ρ_{ab}.

Conversely, now consider two monobots that are initially uncorrelated so that their joint covariance is

$$\Sigma = \begin{bmatrix} \sigma_a^2 & 0 \\ 0 & \sigma_b^2 \end{bmatrix}.$$

Assume that this system is able to measure the relative range between the two monobots as modeled by

$$z = \mathrm{H}\mathbf{x} + v, \quad \mathrm{H} = \begin{bmatrix} 1 & -1 \end{bmatrix}$$

with measurement noise $v \backsim \mathcal{N}(0, \sigma_r^2)$. Again, after applying the standard Kalman update, the resulting covariance matrix is

$$\Sigma' = \frac{1}{\sigma_a^2 + \sigma_b^2 + \sigma_r^2} \begin{bmatrix} \sigma_a^2(\sigma_b^2 + \sigma_r^2) & \sigma_a^2\sigma_b^2 \\ \sigma_a^2\sigma_b^2 & \sigma_b^2(\sigma_a^2 + \sigma_r^2) \end{bmatrix},$$

showing that correlation has been established between the two vehicles where previously it had not existed.

References

[1] M. Hunt, W. Marquet, D. Moller, K. Peal, W. Smith, and R. Spindel, "An acoustic navigation system," Woods Hole Oceanographic Institution, Tech. Rep. WHOI-74-6, Dec. 1974.

[2] R. M. Eustice, L. L. Whitcomb, H. Singh, and M. Grund, "Recent advances in synchronous-clock one-way-travel-time acoustic navigation," in Proc. IEEE/MTS OCEANS Conf. and Exhib., Boston, MA, USA, 2006, pp. 1–6.

[3] J. Vaganay, J. Leonard, J. Curcio, and J. Willcox, "Experimental validation of the moving long base-line navigation concept," in Autonomous Underwater Vehicles, 2004 IEEE/OES, june 2004, pp. 59–65.

[4] S. E. Webster, R. M. Eustice, H. Singh, and L. L. Whitcomb, "Preliminary deep water results in single-beacon one-way-travel-time acoustic navigation for underwater vehicles," in Proc. IEEE/RSJ Intl. Conf. Intell. Robots Systems, St. Louis, MO, Oct 2009, pp. 2053–2060.

[5] M. F. Fallon, G. Papadopoulos, J. J. Leonard, and N. M. Patrikalakis, "Cooperative auv navigation using a single maneuvering surface craft," The International Journal of Robotics Research, vol. 29, no. 12, pp. 1461–1474, 2010.

[6] A. Bahr, M. R. Walter, and J. J. Leonard, "Consistent cooperative localization," in Proc. IEEE Intl. Conf. Robotics and Automation, ser. ICRA'09. Piscataway, NJ, USA: IEEE Press, 2009, pp. 4295–4302.

[7] S. E. Webster, L. L. Whitcomb, and R. M. Eustice, "Preliminary results in decentralized estimation for single-beacon acoustic underwater navigation," in Proc. Robotics: Science and Systems Conf., Zaragoza, Spain, June 2010.

[8] J. Partan, J. Kurose, and B. N. Levine, "A survey of practical issues in underwater networks," SIGMOBILE Mob. Comput. Commun. Rev., vol. 11, no. 4, pp. 23–33, 2007.

[9] H. C. Brown, A. Kim, and R. M. Eustice, "Development of a multi-AUV SLAM testbed at the University of Michigan," in Proc. IEEE/MTS OCEANS Conf. and Exhib., Quebec, Canada, Sep. 2008, pp. 1–6.

[10] S. E. Webster, "Decentralized single-beacon acoustic navigation: Combined communication and navigation for underwater vehicles," Ph.D. dissertation, Johns Hopkins University, Baltimore, MD, 2010.